PNAS RESEARCH ARTICLE | EVOLUTION

The genome of the black-footed cat: Revealing a rich natural history and urgent conservation priorities for small felids

Jiaqing Yuan[a], Andrew C. Kitchener[b,c], Laurie Bingaman Lackey[d,1], Ting Sun[a], Qigao Jiangzuo[e], Yilamujiang Tuohetahong[a], Le Zhao[a,f], Peng Yang[a], Guiqiang Wang[a], Chen Huang[a], Jinhong Wang[a], Wenhui Hou[a], Yang Liu[a], Wu Chen[g], Da Mi[h,i], William J. Murphy[j], and Gang Li[a,g,2]

Edited by Elaine Ostrander, National Human Genome Research Institute, Bethesda, MD; received June 27, 2023; accepted October 31, 2023

Habitat degradation and loss of genetic diversity are common threats faced by almost all of today's wild cats. Big cats, such as tigers and lions, are of great concern and have received considerable conservation attention through policies and international actions. However, knowledge of and conservation actions for small wild cats are lagging considerably behind. The black-footed cat, *Felis nigripes*, one of the smallest felid species, is experiencing increasing threats with a rapid reduction in population size. However, there is a lack of genetic information to assist in developing effective conservation actions. A de novo assembly of a high-quality chromosome-level reference genome of the black-footed cat was made, and comparative genomics and population genomics analyses were carried out. These analyses revealed that the most significant genetic changes in the evolution of the black-footed cat are the rapid evolution of sensory and metabolic-related genes, reflecting genetic adaptations to its characteristic nocturnal hunting and a high metabolic rate. Genomes of the black-footed cat exhibit a high level of inbreeding, especially for signals of recent inbreeding events, which suggest that they may have experienced severe genetic isolation caused by habitat fragmentation. More importantly, inbreeding associated with two deleterious mutated genes may exacerbate the risk of amyloidosis, the dominant disease that causes mortality of about 70% of captive individuals. Our research provides comprehensive documentation of the evolutionary history of the black-footed cat and suggests that there is an urgent need to investigate genomic variations of small felids worldwide to support effective conservation actions.

black-footed cat | introgression | conservation | inbreeding

Cats (Family Felidae) have evolved a conservative body plan as specialized predators of mostly vertebrates (1). Most species hunt their prey in a wide range of habitats using a stealthy approach (stalking) followed by an explosive burst of speed to capture their prey. However, human activities, such as habitat loss and hunting for fur, have an increasingly negative impact, threatening the survival of all wild cat species. The largest cats, like the tiger (*Panthera tigris*), leopard (*P. pardus*), and cheetah (*Acinonyx jubatus*), etc., receive considerable global attention and high levels of conservation funding linked to more comprehensive international protection. There are also considerable genetic data available for larger cat species, which provides important information about their evolution and the genetic consequences of human impacts that inform conservation actions. However, these data are generally lacking for small cat species, where even basic ecological data are either sparse or lacking.

The little-known black-footed cat (BFC), *Felis nigripes*, is one of the smallest (less than 1.93 kg) (2) species in the Felidae. The BFC avoids competition with and direct predation by larger predators through its strictly nocturnal behavior, which has been revealed in recent field studies using radiocollars (3, 4). The BFC has a remarkably high hunting success of ~60% (5), so it can maintain high activity levels throughout the night. Correspondingly, the BFC has a high metabolic rate, which requires the consumption of ~20% of its body weight per day to maintain energy levels (6, 7).

The BFC currently occupies arid regions of southern Africa from South Africa to Botswana, Namibia, and Zimbabwe (2) (Fig. 1*A*). Disproportionate to their small body sizes, both female and male BFCs occupy relatively larger home ranges compared to other larger felids (Fig. 1*B* and *SI Appendix*, Table S1). Faced with anthropogenic threats, such as habitat loss and fragmentation, there has been a fast decline in population, estimated locally as almost 50% during a long-term study over 20 y (4). Habitat fragmentation, leading to the isolation of subpopulations, may exacerbate reductions in genetic variability and increase levels of inbreeding in some populations. However, there is a paucity of genetic data about the BFC, so that much is still unknown about its evolutionary history, genetic diversity, and inbreeding risk.

Significance

Although all felid species are impacted by habitat loss and human activities. Conservation efforts for small felid species lag significantly behind their larger counterparts in the Felidae family, highlighting the need for greater attention and resources. Recognizing the critical role of conserving these felids is paramount for preserving species diversity. Our research focuses on the genomic analysis of the black-footed cat, elucidating its evolutionary history and genetic adaptations. Alarming levels of inbreeding within the black-footed cat population, likely resulting from habitat fragmentation, intensify the risk of amyloidosis, a prominent and fatal disease associated with deleterious mutations. This research underscores the urgency of investigating genomic variations and formulating effective strategies for small felids, which are integral to ecological balance and biodiversity.

The authors declare no competing interest.

This article is a PNAS Direct Submission.

[1]Retired.

[2]To whom correspondence may be addressed. Email: gli@snnu.edu.cn.

This article contains supporting information online at https://www.pnas.org/lookup/suppl/doi:10.1073/pnas.2310763120/-/DCSupplemental.

Published January 2, 2024.

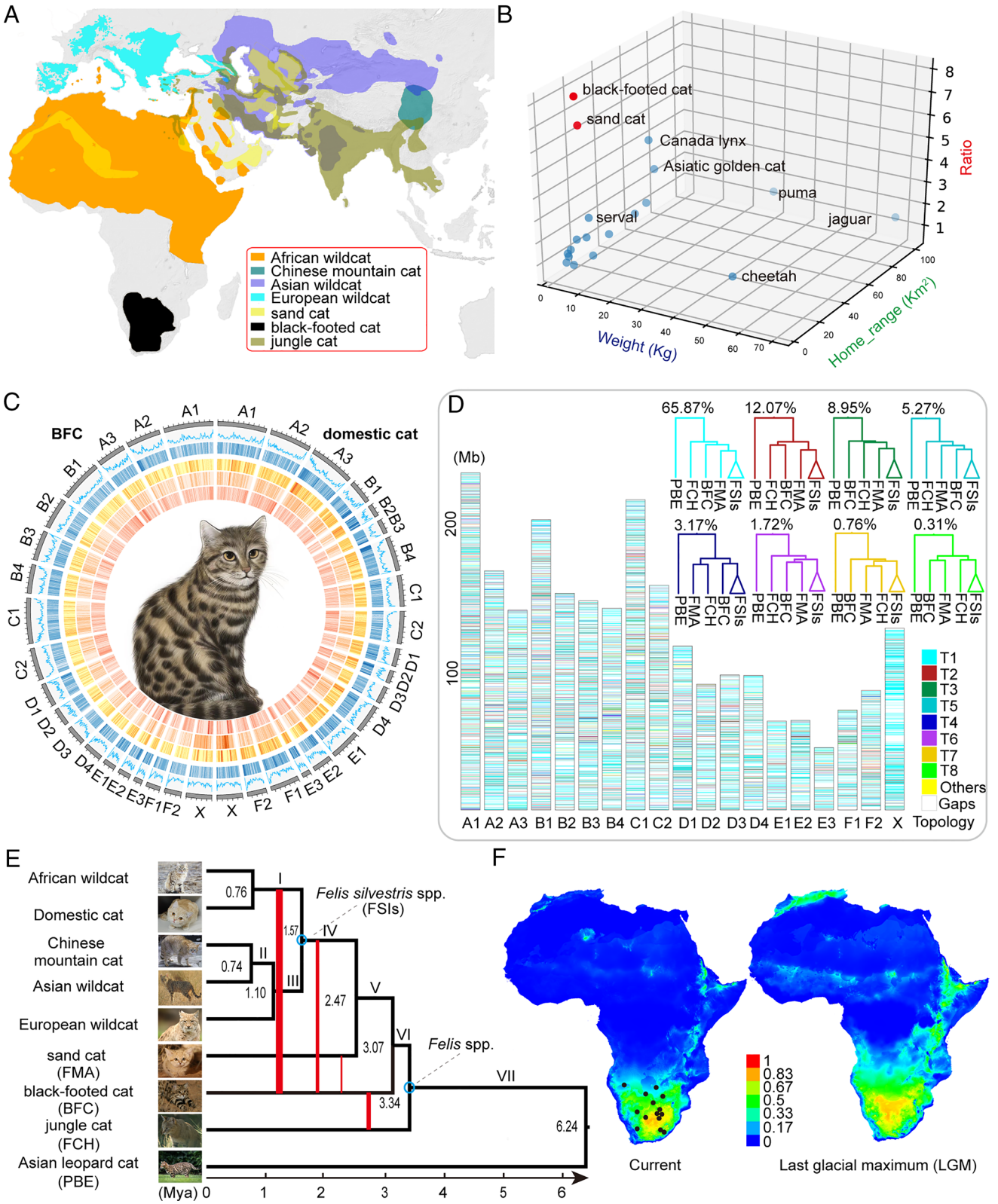

Fig. 1. Phylogeny of *Felis*. (*A*) The geographical distribution of current *Felis* species based on IUCN data. (*B*) The distribution of the ratio (*Z* axis) of home range size (*Y* axis) to weight (*X* axis) shows *F. nigripes* is the highest among Felidae species. (*C*) Circos plots between the domestic cat (*Right*) and the BFC (*Left*). The circles from outside to inside represent karyotypes, GC contents, gene density, and repeats elements (LINE, SINE, LTR), respectively. (*D*) Each bar represents a chromosome of the domestic cat (felcat9.0). Colored bands represent tree topologies of 50-kb per window; colors correspond to the upright topologies, with white regions showing missing data. (*E*) The reconstructed time-scaled species tree of the genus *Felis* with Asian leopard cat, *Prionailurus bengalensis*, as outgroup. Colored lines represent the introgression between the BFC and other *Felis* species. (*F*) The schematic shows the current distribution area of the BFC (*Left*) and the estimated historically adaptative geographic space according to the historical climate conditions in the last glacial maximum period (*Right*). The black dots represent the locations of the observations of the BFCs, and the color bar indicates gradient of the probability of presence in the BFCs.

Severe mortality of about 70% of captive individuals of the BFC has been caused by amyloidosis (8), even though amyloid is present in wild BFC populations (8). Amyloidosis is caused by fibrillar protein depositions in many organs, and studies in animal models demonstrate that this disease has a genetic basis. Research has shown a much higher probability of amyloidosis in inbred mice than in non-inbred mice (9). Therefore, the BFC may face a combined crisis of high levels of inbreeding, which are still unknown, with a probable risk of amyloidosis affecting wild populations, that calls for field surveys. It has been speculated that the type of amyloidosis in BFCs is inherited, which requires more comprehensive genetics research.

To understand the evolutionary history, unique genomic adaptations, and assessment of current genetic risks of the BFC, we generated a high-quality chromosome-level reference genome from a female individual and collected samples from nine non-related BFCs (*SI Appendix*, Fig. S1) to generate the whole genome resequencing data (>20X genomic coverage for each one). Combined with the previously published genomic data of the BFCs and all other *Felis* species (31 genomic data) (*SI Appendix*, Table S2), we carried out genomic comparisons and population genomics research on this very small cat species.

Results

Genomic Sequencing, Assembly, and Annotation. A total of ~265 GB genomic sequencing data were used for the high-quality de novo genome assembly of the BFC, including 80.51 GB of PacBio long reads, 80.24 GB of Illumina paired-end short reads, and 104.8 GB Hi-C reads (*SI Appendix*, Table S2). The de novo genome assembly constructed 446 contigs with long-sequence contiguity (N50 equals to 37.19 Mb), which were anchored to 19 chromosomes (Fig. 1*C* and *SI Appendix*, Fig. S2 and Table S3). This assembled reference genome has a genome size of 2.46 GB with high genome completeness [97.6% by BUSCO test and 53 of quality value (QV)]. The results of genome annotation present 790.68 Mb (32.14%) of repetitive sequences and 20,470 protein-coding genes within the BFC genome (*SI Appendix*, Tables S4 and S5). The gene function annotations with non-redundant (NR) and UniProt databases are up to 20,389 (99.60%) and 19,299 (94.28%), respectively (*SI Appendix*, Table S5). The results of genome comparison between the BFC and domestic cat, *Felis catus* (felCat 9.0), involving chromosomal variation, GC content, gene density, and repeat sequences (SINE, LINE, and LTRs), are depicted in Fig. 1*C*. To better understand the genetic variations of the BFCs on population level, we generated ~570 Gb Illumina paired-end short reads data of nine individuals of the BFCs, with approximately 20X whole genome coverages for each individual.

Phylogenomic Analysis. To investigate variation in genome-wide phylogenetic signals in the genus *Felis*, we applied continuous sliding window scanning across the whole-genome alignment matrix of the BFC, jungle cat (*Felis chaus*), sand cat (*Felis margarita*), domestic cat/wildcats group (European wildcat (*Felis silvestris*), Asian wildcat (*Felis ornata*), Chinese mountain cat (*Felis bieti*), North African wildcat (*Felis lybica*) and domestic cat (*Felis catus*), as well an outgroup of the Asian leopard cat (*Prionailurus bengalensis*) (*SI Appendix*, Table S6). After filtering repetitive sequences and alignment gaps, the final ~601 Mb of aligned genomic data shared by all nine taxa were used to reconstruct phylogenetic trees. The summarized results of all non-overlapped sliding-window (50-kb window size) trees produced more than 928 different highly supported tree topologies (>70% bootstrap of all nodes), indicating massive signals of phylogenetic discordance in *Felis* (Fig. 1*D* and *SI Appendix*, Fig. S3). Without considering the phylogenetic complexity within the domestic cat/wildcat lineage, the dominant topology was supported by 65.9% (13,730/20,846) of all sliding windows (T1 in Fig. 1*D*) and the seven additional tree topologies covered from 12.1 to 0.3% of all sliding tree topologies (Fig. 1*D*).

We performed additional phylogenetic analyses of the coding gene sequence matrix, including nucleotide and protein sequences of one-to-one single copy orthologues from all sampled felids genomes, to construct a bifurcating species tree (*SI Appendix*, Fig. S4). All of these approaches produced identical tree topologies to the dominant tree reconstructed by the sliding windows test (T1 topologies), which we used as the species tree for divergence time estimation. We used the concatenated genome data of sliding windows possessing T1 signals to estimate a time tree for the genus *Felis*. Our results show that the jungle cat diverged first from the *Felis* lineage around 3.34 (CI = 2.10 to 4.78) Mya, followed by the BFC (3.03 Mya, CI = 1.94 to 4.40 Mya) and the sand cat (2.47 Mya, CI = 1.54 to 3.55 Mya). The domestic cat/wildcat group formed two clades about 1.57 Mya; the first clade comprises the European wildcat, Asian wildcat, and Chinese mountain cat, while the second clade includes African wildcat and domestic cat Fig. 1*E*.

Introgression of BFC. To disentangle whether phylogenetic discordance among *Felis* taxa has resulted from introgression or incomplete lineage sorting (ILS) as was previously reported (10), we conducted a series of tests using different software [Dsuite (11), QuIBL (12), and ANGSD (13)] with independent algorithms based on input data of sequences or phylogenetic trees.

Patterson's *D* statistics with Dsuite or ANGSD showed that *Felis* went through more than 10 introgression events (*SI Appendix*, Tables S7 and S8). While these introgression events could not completely explain all of the phylogenetic discordance, we performed additional introgression tests, using the method "quantifying introgression via branch lengths" [QuIBL (12)] to focus on introgression between the BFC and other *Felis* species. We took the triplet (jungle cat, BFC, and sand cat) with Asian leopard cat as the outgroup to detect potential introgression or ILS, which may cause topology 2 (T2) in Fig. 1*D*. The results of this test support an introgression event between the BFC and the jungle cat (Fig. 1*E*). A similar test of the triplet (BFC, sand cat, and domestic cat) showed that the ancestors of the BFC and the sand cat went through an ancient introgression event (Fig. 1*E* and *SI Appendix*, Table S9). In addition, species distribution modeling analysis of BFC at the Last Glacial Maximum (LGM) showed that the BFC extended its range to a broader East African region compared to its current distribution (Fig. 1*F*).

Adaptive Evolution. To further study the adaptive evolution of the BFC, a pipeline of comparative genomics analyses was performed on five cat species, including the BFC, jungle cat, domestic cat, Asian leopard cat, and Canada lynx, for which high-quality genome data are available. We applied the software Orthofinder (14) to identify 20,477 homologous groups of gene families (*SI Appendix*, Table S10). Compared to other *Felis* species, 43 expanded gene families, including 106 genes, were identified on the BFC branch (Fig. 2*A*), the functions of which are significantly ($P < 0.05$) enriched to the KEGG pathway items of immunity or local disease, such as African trypanosomiasis. (Fig. 2*B* and *SI Appendix*, Table S11).

Testing for signatures of natural selection, we identified 113 positively selected genes (PSGs) and 319 rapidly evolved genes (REGs) in the BFC lineage (*SI Appendix*, Tables S12 and S13).

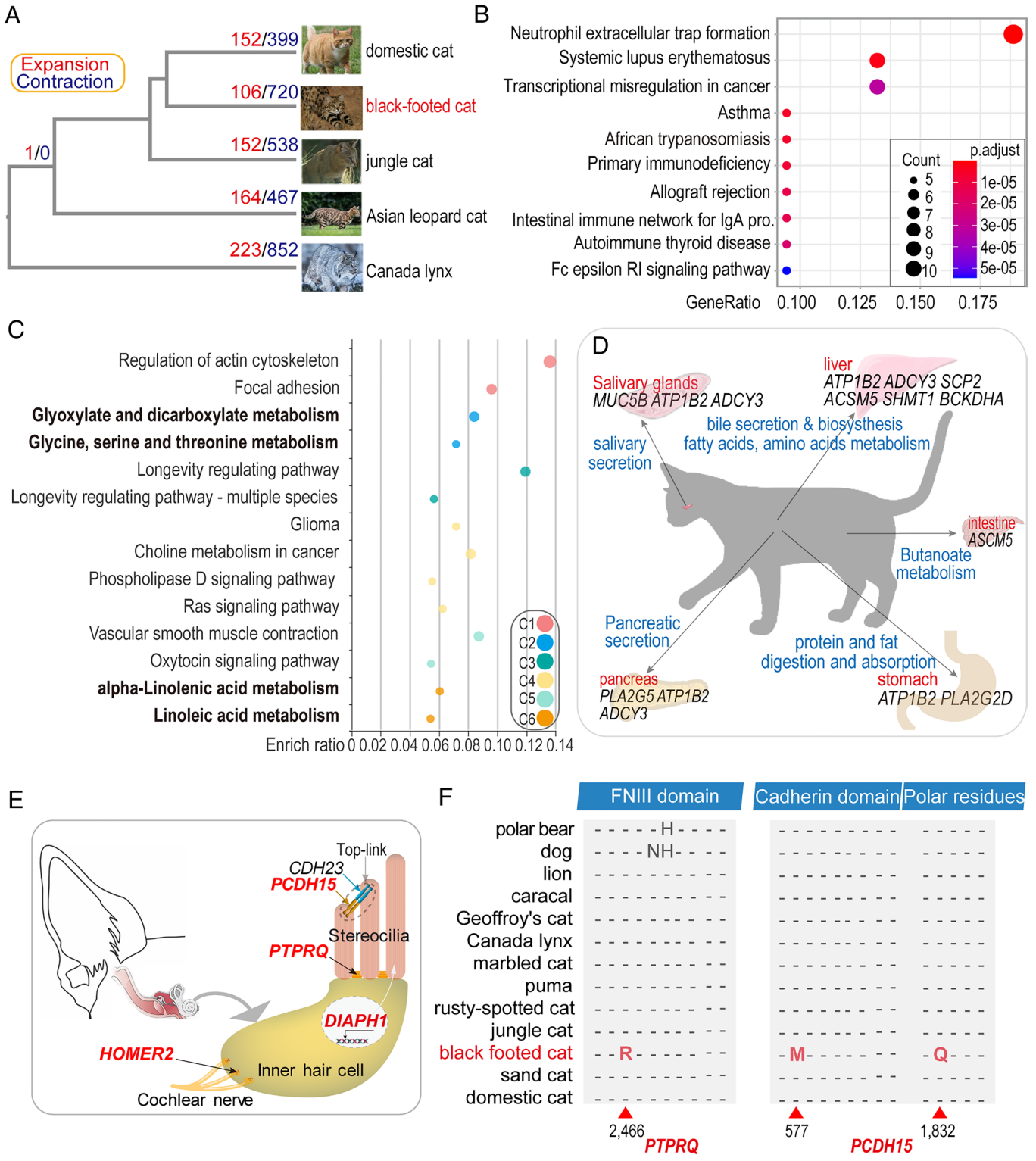

Fig. 2. Genomic signatures of genetic adaptation in the BFC. (*A*) Gene family expansion/contraction of the compared species of the genus *Felis* and outgroups. (*B*) KEGG enrichment items of the expanded family genes in BFC. (*C*) The results of KEGG functional enrichment test of detected PSGs and REGs. (*D*) The metabolic related functional genes with the tested significant selection signals in digestive system BFC. (*E*) Three PSGs have defined functions in stereocilia connections and mechanosensory transduction (*PCDH15* and *PTPRQ*) and regulation of actin polymerization within stereocilia (*DIAPH1*), while one REG (*HOMER2*) is a receptor involved in transduction of nerve impulses. (*F*) BFC-specific amino acid mutations at the conserved structures (FNIII: Fibronectin type III domain, cadherin domain, and Polar residues) in *PCDH15* and *PTPRQ* genes compared with different felid species and outgroups. These two genes are involved in the function of inner hair cells' stereocilia movement.

The result of KEGG tests suggested the functions of these genes are significantly ($P < 0.05$) enriched to the regulation of actin cytoskeleton, Fanconi anemia pathway, longevity regulating pathway, ovarian steroidogenesis, metabolic pathways, glycine, serine and threonine metabolism, linoleic acid metabolism, etc. (Fig. 2*C* and *SI Appendix*, Tables S14–S16).

The BFC is a highly active nocturnal hunter and is reported to have a high metabolic rate among cats (6, 7). We identified a series

of PSGs or REGs and their functions are significantly associated with fat and protein metabolism (Fig. 2*D* and *SI Appendix*, Tables S14–S16). For example, the butanoate metabolism–related gene *ACSM5,* is involved in the digestion of short chain fatty acids in the intestine, as well as four genes *ACSM5*, *SCP2*, *SHMT1,* and *BCKAHA*, which are all involved in pathways of fat and protein metabolism.

The BFC possesses sensitive visual capabilities and one of the largest ratios of auditory bulla size to body size among extant felids (5, 15–17). Several sensory genes, such as the vision gene *OPN1SW*, and hearing-related genes, *PCDH15*, *PTPRQ*, *AKNAD1*, *DIAPH1*, *MYO18B*, and *HOMER2* (from https://hereditaryhearingloss.org) were detected with significant signals of positive natural selection or rapid evolution in the BFC (Fig. 2*E* and *SI Appendix*, Fig. S5 and Table S16).

Genetic Diversity Analysis. The results of the principal components analysis (PCA) and phylogenetic tree building revealed the genetic separation between the BFCs and other *Felis* spp. (Fig. 3*A* and *SI Appendix*, Fig. S6). To identify unique selection sweeps within the BFC compared with those of other *Felis* species, we performed population tests to scan the population genomic data of 15 BFCs versus those of 23 genomic data of the other three *Felis* species/subspecies. Given the results of the analysis, we identified 379

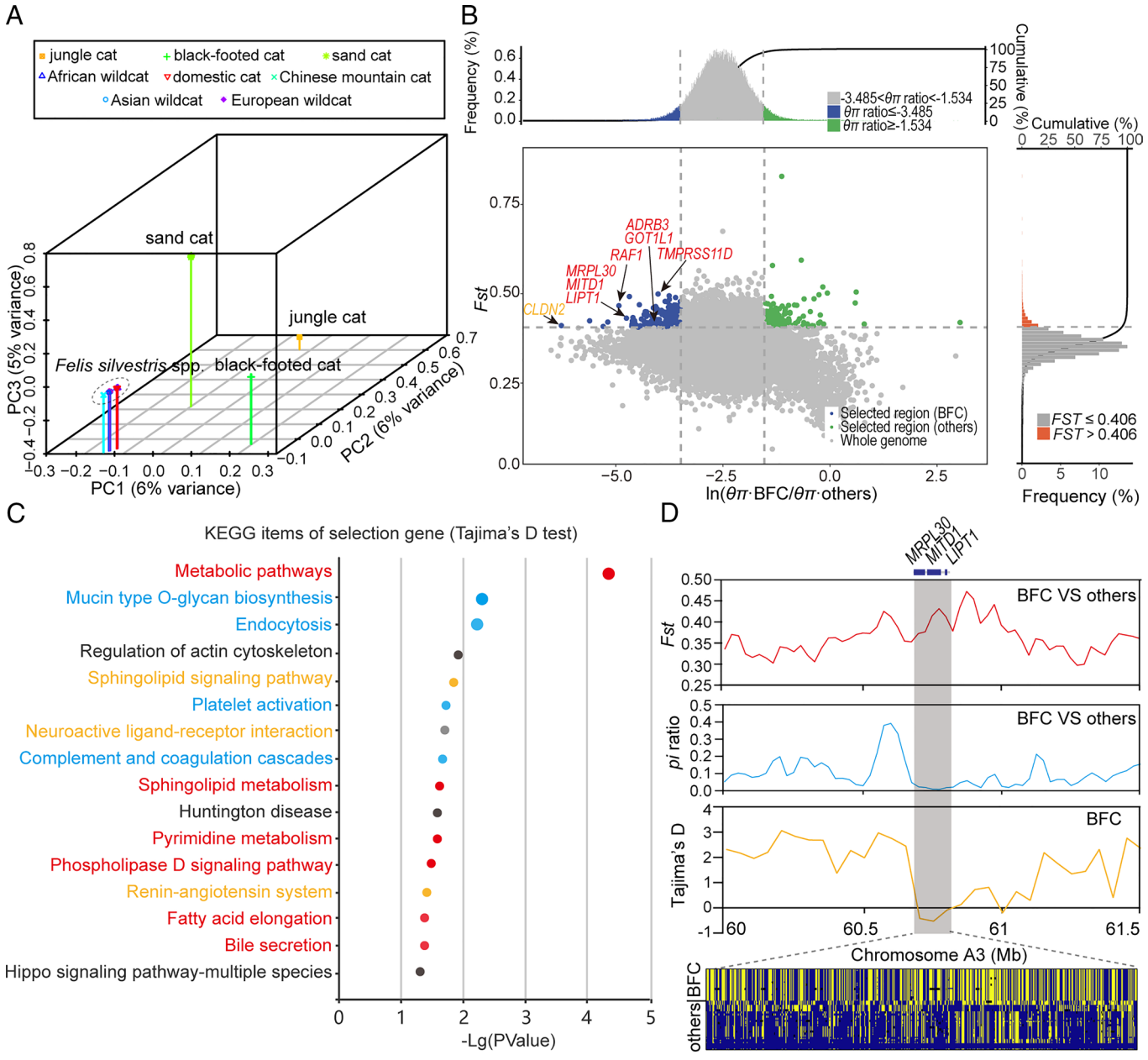

Fig. 3. A comparison of genomic selection between the BFC and other *Felis* species. (*A*) Plots of principal components 1, 2, and 3 from PCA analysis of *Felis* spp. (*B*) Distribution of ln (pi ratios) and *Fst* values calculated in 50-kb sliding windows with 25-kb increments between BFCs group and control group (including jungle cat, sand cat, and other five wildcat species). The data points in blue [corresponding to the top 5% of the empirical ln(pi ratios) distribution with values < = -3.485 and the top 5% of the empirical *Fst* distribution with values > 0.406] are genomic regions under selection in BFC group. (*C*) The top 20 KEGG pathways were identified by the functional enrichment tests on genes that are under selection from Tajima's D test, and the most significant item is the metabolic pathway (*P*: 4.76E-05). The KEGG items with different colors were associated with metabolism (red), immune (blue), and nervous system (orange). (*D*) A region with significant genetic divergence and selection (*Fst* = 4.793 and π ratio = 2.652) between BFC and other contains three genes: *MRPL30*, *MITD1* and *LIPT1*, and the pattern of genotypes shows the different between BFC (major allele) in yellow and others (minor allele) in blue.

and 1,900 candidate genes located in regions that were detected with the highest divergence (top 1% of *Fst* values cutoffs, *Fst* > 0.437; top 5% of *Fst* values cutoffs, *Fst* > 0.406) between the BFC and other *Felis* species, and the results of KEGG enrichment tests suggested the function of these genes are significantly (P < 0.01) associated with the metabolic pathways (*SI Appendix*, Fig. S7 and Tables S17–S20). We further carried out pairwise nucleotide diversity ($\theta\pi$) tests. The results identified 291 regions (including 129 genes) that were significantly diverged between the BFCs and other *Felis* spp., supported by both *Fst* (*Fst* > 0.406, top 5% level) and $\theta\pi$ [$\log_2(\theta\pi$ ratio) < −3.485, top 5% level] tests. The further gene functional enrichment tests showed that the function of these 129 genes was significantly (P < 0.01) associated with the thyroid hormone signaling pathway, Fanconi anemia, and nitrogen metabolism, as well the regulation of lipolysis in adipocytes, which are linked to the bioprocess of energy metabolism (Fig. 3*B* and *SI Appendix*, Tables S21 and S22). In addition, we also conducted the Tajima's D tests and the results of this analysis found 941 regions with the Tajima's D values lower than zero. The results of the gene functional enrichment test on 432 genes within these regions also provided the strongest signals of relative metabolic functions (Fig. 3*C* and *SI Appendix*, Tables S23 and S24). Finally, combined with all results of *Fst*, $\theta\pi$, and Tajima's D test, we identified 27 shared regions from 18 genes of the BFCs were strongly diverged from the back group of other *Felis* spp. (*SI Appendix*, Table S25). For instance, a region adjacent to 61 Mb on chromosome A3, including genes of *MRPL30* (mitochondrial ribosomal protein L30) and *LIPT1* (lipoyltransferase 1), is functionally involved in energy metabolism (Fig. 3*D*).

Demographic History and Genomic Diversity. A pairwise sequential Markovian coalescent (PSMC) model was used to trace the demographic histories of *Felis* species (Fig. 4*A*). The results revealed that BFC has the almost lowest effective population size within the past 300,000 y (Ky) within the genus *Felis* (excepting only the sand cat). Unlike major population expansions that occurred around 60 Kya (within the last interglacial period) in most *Felis* species, the BFC population experienced a continuing long-term decline in population size. However, a slight population expansion of the BFC may have occurred around 20 Kya just after the peak of the LGM.

We compared average heterozygosity of the BFC with that of other *Felis* species, which showed that the BFC and the sand cat have the lowest level of heterozygosity which are even lower than those of major the big cat species of the genera *Panthera* and *Puma* (Fig. 4*B* and *SI Appendix*, Table S26), as well as higher fraction of runs of homozygosity (FROH) (Fig. 4 *B* and *C* and *SI Appendix*, Table S27). ROH fragments with different lengths can reflect a gradient of inbreeding history. In our study, all the analyzed BFC individuals were detected with a high level of ROH in their genomes (535 Mb to 1.07 Gb) which were widely distributed on each chromosome in genome (Fig. 4*D* and *SI Appendix*, Fig. S8).

Deleterious Mutations Associated with Amyloidosis. To understand the current impact of amyloidosis, which is the major cause of mortality in captivity, we targeted variants within genes that are related to this disease in the population genomic data of the BFCs. By gene database searching (https://www.ncbi.nlm.nih.gov/gene), we set a gene group including 77 annotated coding genes which were reported functionally to involve the disease of amyloidosis. In this group of genes, we found the frequent presence of missense mutations, including 67 alleles of 29 genes (Fig. 4*E* and *SI Appendix*, Tables S28 and S29). It is worth noting that BFCs carried a missense deleterious mutation (Gly to Ser) in a gene previously linked to amyloidosis (*TRR*) (18–20) (Fig. 4*F*). In addition, *TTR* and a second gene *B4GALT6*, which are also strongly linked to amyloidosis in mice and human (21, 22), are located in the ROH region of the BFC. Moreover, a missense deleterious mutation (alanine to glycine) on the 37th amino acid site of another gene related to amyloidosis (*BACE1*) was found in the BFC. Protein-sequence alignment suggested this gene is extremely conserved across all representative mammalian species (*SI Appendix*, Fig. S9). A functional prediction test performed with SIFT, suggested the BFC-specific mutations cause potential functional change of protein.

Discussion

Phylogeny of *Felis*. The historical and current geographical distributions of *Felis* spp. are correlated with their phylogenetic relationships that were reconstructed in our study using genomic data. The common ancestor of the genus *Felis* is inferred to be of East Asian origin from the characters of the oldest known fossil *Felis* from the Mazegou Formation of the Yushe Basin, Shanxi (3.7 to 2.8 Ma), China, which is similar to the modern jungle cat (23, 24). This was the first species to split from the *Felis* lineage within this genus and currently extends westward from South Asia to Egypt in North Africa (25). The distribution of the BFC is restricted to a limited area in southern Africa (26), while the sand cat is in South West Asia and North Africa (27). The estimated divergence time (~2.47 Mya) between the sand cat and wildcats occurred in the early Pleistocene (~2.58 to 0.773 Mya) (28), when severe cyclical climate change was caused by repeated alternation of ice ages (29–31). The oldest wildcat fossil (*Felis lunensis* Martelli, 1906) has been recorded from the late Pliocene to early Pleistocene (c.1.5-2.0 Mya) in several sites across Europe (1, 32), which is consistent with the estimated divergence time between sand cats and the wildcat lineage. Our results supported two clades within the wildcats' group, which may have diverged approximately 1.57 Mya. One clade includes the European wildcat (*Felis silvestris*), the Asian wildcat (*Felis ornata*), and the Chinese mountain cat (*Felis bieti*). Long-term cooling during the mid-Pleistocene transition (~1.2 to 0.7 Mya) led to the expansion of the semi-deserts and steppes in Asia (33, 34), which coincided with the estimated divergence time of European wildcats from the common ancestor of Asian wildcats and Chinese mountain cats at approximately ~1.10 Mya. The current geographical distribution of Asian wildcats and Chinese mountain cats are closer and overlap in northern China (Fig. 1*A*). The second clade is composed of African wildcats and includes domestic cats, which is consistent with previous research that showed that domestic cats originated from North African/Near Eastern wildcats (35).

The intricate pattern of hybridization among *Felis* species throughout their evolutionary history is one of the main reasons for observed phylogenetic discordance (10, 36, 37). Rapid species radiation and lack of sufficient time to establish genetic isolation and divergence, together with overlaps of historical distribution between species, may have led to frequent introgression events among ancestors of the *Felis* species. In our study, we detected introgressions between the BFC and the respective ancestors of the jungle cat, sand cat, and wildcats. The results of the historical distribution modeling tests for the BFC suggested that the geological regions with suitable climatic conditions for the BFC could have expanded to Eastern Africa in the LGM, which we speculate were sympatric with the African wild cat, and contributed to the observed genome introgressions between these two groups (Fig. 1*F*).

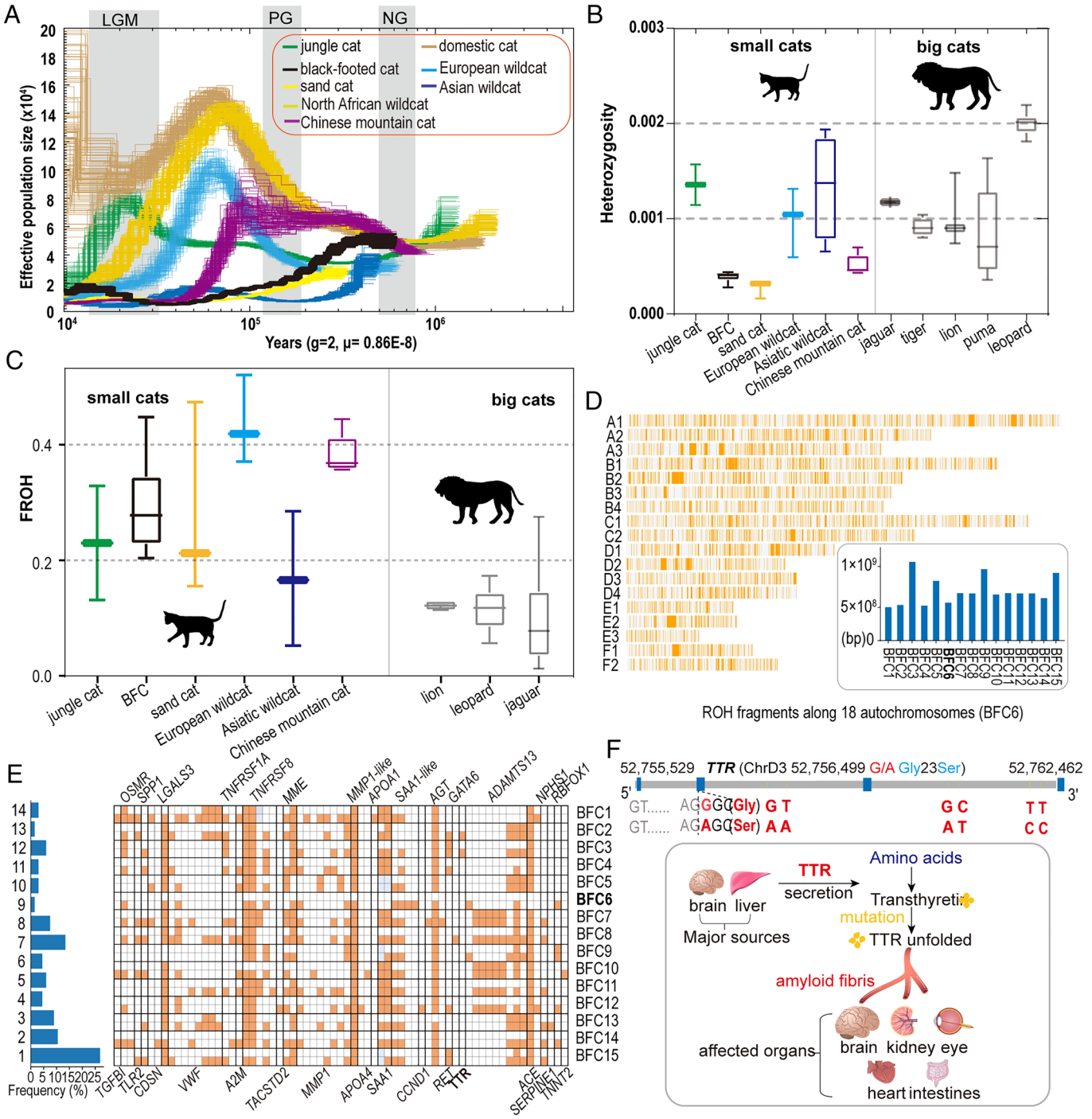

Fig. 4. Conservation genetics of the BFC. (*A*) PMSC analysis of the population history of eight *Felis* species during three major glacial periods, i.e. the LGM, Penultimate Glacial (PG) and Naynayxungla Glaciation (NG). (*B*) The levels of heterozygosity (*Left*) of small *Felis* species and big cats (*Right*). (*C*) The levels of FROHs (*Left*) of small *Felis* species compared with those of three big cats (*Right*). (*D*) The histogram exhibits the total ROH lengths of all 15 BFCs, and the landscape of the distribution of ROH fragments on 18 autosomes of the BFC individual BFC6 which was used for de novo genome assembly. (*E*) The 67 alleles of missense mutations detected in 29 amyloidosis-associated genes carried by 15 BFCs. The red colored boxes represent the missense SNPs compared with the reference genome of the BFC. The histogram at left shows the frequencies of the mutated alleles in 67 alleles of 15 BFCs. (*F*) The gene structure of TTR contains four exons in BFC with four SNPs. The missense deleterious mutation (ChrD3 52,756,499 G/A Gly23Ser) found at the first position of codon23 in the second exon of the *TTR* gene. The bottom diagram simply shows the process that abnormal deposits of TTR protein in various tissues and organs throughout the body.

Adaptive Evolution of the BFC. The BFC is a strictly nocturnal hunter (3, 5), which may allow it to avoid competition for resources and escape from predation by larger carnivorans (3, 26, 38). The BFC's excellent senses of hearing and sight allow it to hunt effectively in almost complete darkness. Compared to other felids, the BFC has a much higher hunting success rate (up to 60%) (5). In our study, a series of sensory genes have signatures of positive natural selection, which may be beneficial for hunting prey. For example, the visual gene *OPN1SW* encodes for a photopigment called S-cone opsin, which is involved in the perception of fast-moving objects (39, 40). Therefore, we speculate that this gene may contribute to effective hunting of small, fast-moving prey (5). The BFC has two classical hunting styles of "slow-hunt" and "sit-down," both of which depend on the ability to detect the slightest sounds or movements from prey (5). For genes associated with hearing, five PSGs (*PCDH15*,

PTPRQ, *DIAPH1*, *AKNAD1*, and *MYO18B*) and one REG of *HOMER2* were detected in the BFC. Damage to these genes causes hearing loss (41–46). *PCDH15* encodes a crucial cadherin of protocadherin-15 to connect stereocilia (41), which are small hair-like structures in the cochlea and are responsible for hearing. The function of *PTPRQ*, also named shaft connectors, involved in stereocilia connections (43), and the products of *DIAPH1* regulate the actin polymerization in inner hair cells (47, 48). *HOMER2* encodes the postsynaptic density scaffolding proteins to regulate signal transduction in the inner hair cells of humans and mice (45). These genes are under significant selections and may have potential importance in enhancing the auditory capabilities of the BFC.

High levels of nocturnal hunting and the need to balance heat loss from a small animal in low temperatures at night require faster and relatively higher energy consumption, so that the BFC's metabolic rate is among the highest in felids (6, 7). Our genome comparisons revealed genetic adaptive evolution of genes that are involved in digestive metabolism, like *ACSM5* (a transport role in cellular lipid absorption) (49), *ANXA9* (fatty acid transporting) (50), *HEXA* (a major regulator of systemic lipid metabolism) (51), and *LIPT1* (glyoxylate metabolism and glycine degradation and metabolism) (52, 53). These results suggest that a suite of genetic adaptations has evolved to support the high metabolic rate of the BFC.

Conservation of the BFC. Compared to big cats, such as tigers, leopards, or cheetahs, ecological and genetic studies of small cats are neglected. In the case of the BFC, we know very little about even basic life history and genetic traits, owing to its small size, scarcity, and secretive nocturnal activities. While based on limited data, a long-term study of the BFC showed a rapid loss of nearly half of the local population size within 20 y (26). The BFC has the most restricted distribution among African felid species (36), and habitat fragmentation, prey loss, and human activities (such as farming practices, bait poisoning, and steel-jaw traps) are crucial threats to their survival. The BFC has the largest home range relative to body size among felids [16.1 to 20.7 km^2 and 8.6 to 10 km^2 of males and female adults (26)], suggesting that prey population density and abundance is low or highly variable, and hence, this species is more vulnerable to habitat loss and fragmentation.

In our study, we have revealed that the BFC has undergone a continuous long-term historical decline in its effective population size. Repeated glacial cycles may have caused this decline, such that it has among the lowest effective population sizes of all *Felis* species during the last 500,000 y. The recent sharp reduction and fragmentation of its habitat caused by human activities may also have contributed to the low genome heterozygosity recorded in our study. Additional evidence of a high frequency of ROHs reflects high levels of inbreeding within BFC populations.

Inbreeding may lead to high incidences of genetic disease (54, 55). Amyloidosis, which is responsible for ~70% of deaths of captive BFCs and has a probable genetic basis (8), is the primary barrier to building an effective captive population for conservation. In our sample of BFCs, we frequently found the presence of missense mutations that occurred in genes associated with to amyloidosis. Two genes, *TTR* and *B4GALT6*, which have previously been associated with amyloidosis (8, 21), are located in a long ROH fragment. More than 130 mutations scattered in the coding region of human TTR gene have been associated with amyloidosis (18), and the missense of Gly23Ser we detected would likely affect protein function by SIFT. Furthermore, the mutation of the exon from GGC to AGC is located next to the exon/intron boundary (GT-AG), which could cause the potential splicing error by completing the normal split site (56, 57). Potentially deleterious mutations of *TTR* were detected in our BFC genome. In addition, the BFC *BACE1* gene, which is also related to amyloidosis (58, 59) possesses a mutation at the 37th amino acid site which is otherwise highly conserved in other placental mammals. Future population-based screening of these variants in a case–control study of captive individuals would be an important next step to identify whether either gene is a causal variant for amyloidosis (58, 59).

Conclusion

Analysis of the genome of the BFC has allowed us to reveal the intricate evolutionary history of the BFC and other cats of the genus *Felis*, as well as possible genetic features that contribute to the adaptive evolution of the BFC. This study highlights the importance of additional genomic studies on other neglected small felids, which may reveal loss of genetic diversity and ancient to recent historic inbreeding leading to an increased frequency of deleterious genetic variation in captive and natural populations. These genomic data will be vital for influencing conservation strategies for small felids throughout the world.

Materials and Methods

Genome Sequencing. The cultured fibroblast cells of a female BFC established by Laboratory of Genomic Diversity, National Cancer Institute, collection was used for whole genome sequencing. Paired-end Illumina sequencing libraries with insert sizes of 350 bp were constructed and sequenced (2 × 150 base pairs, bp) on the Illumina NovaSeq 6000 platform.

High-quality genomic DNA was extracted from muscle tissue using the Magnetic Animal Tissue Genomic DNA Kit (TIANGEN), using a modified cetyltrimethylammonium bromide (CTAB) method. Genomic DNA was sheared to a size of 40 kb, using a Megaruptor (Diagenode) device (Belgium), and was then used for single-molecule real-time (SMRT) library preparation as recommended by PacBio. Scaffolding was performed with publicly available Hi-C reads from DNA Zoo (60, 61).

We collected nine BFC samples of zoo origin from National Museums Scotland. DNA samples used for whole genome resequencing were extracted from the muscle tissue using the Magnetic Animal Tissue Genomic DNA Kit (TIANGEN). Sequence libraries were constructed using the Novogene NGS DNA library prep set (Cat No.PT004)*. The sequencing works were performed using the platform of Illumina NovaSeq 6000.

Genome Assembly of BFC. All PacBio sequences provided by Maryland Genomics (University of Maryland, institute for genome sciences) were conducted by fastqc (v0.11.9) with default parameters and fastp (v0.20.1) with the parameters of "-5 -W 5 -M 30 -q 30 -z 1 -n 5" and then were corrected by NEXTDENOVO (v2.4.0) (https://github.com/Nextomics/NextDenovo) with default parameters and assembled using Flye (v2.8.1-b1676) (62) with parameters "--nano-raw --iterations 2." Assembled contigs were further polished by NextPolish (v1.3.1) (https://github.com/Nextomics) with minimap2_options parameter "-x map-ont" for three rounds using Illumina reads. Redundant sequences were identified and removed using PURGE_DUPS (v1.2.5) (https://github.com/dfguan/purge_dups). The assembled contigs with Hi-C data, downloaded from DNAZoo (*SI Appendix*, Table S2), were used to construct the chromosome-level assembly. Final assembly was curated manually with Juicebox (v1.9.8) (61). Benchmarking Universal Single-Copy Orthologs (BUSCO) (v4.1.2) (63) was used to evaluate the completeness of the gene sets in our draft genome. We also performed the evaluation of assembly quality with Quality Value (QV) score, which was calculated using the formula QV = $-10*\log_{10}$(substitution_number/genome_size).

Mapping to Construct Assemblies. Paired-end reads of five *Felis* spp. (sand cat, European wildcat, Chinese mountain cat, Asian wildcat, and African wildcat) were mapped to those of their close relative with a high-quality assembly genome, the domestic cat (GCF_018350175.1) with the bwa mem algorithm (64) and samtools/bcftools (v1.1) (65) with its consensus algorithm, to generate five consensus

genomes. The detailed commands are "samtools mpileup -uf reference.fa bam.file | bcftools call -mv -Oz -o vcf.out" and "cat reference.fa | bcftools consensus vcf.out > consensus.genome.fa."

Annotation. Repetitive sequences and transposable elements in the above assembly of the BFC genome were detected by a combination of de novo and homology-based approaches. Repeatmasker (v4.0.7) (http://www.repeatmasker.org/) with the parameters of "-e ncbi -gff -xsmall -species Carnivora" was used to identify repeats based on homology predictions with the Repbase database (v 2017-01-27) of known repeats in Carnivora. RepeatModeler (v1.0.11, http://www.repeatmasker.org/RepeatModeler/) with the parameters of "-database species -LTRStruct" was applied to construct the de novo repeat custom library, which was used to predict repeats by Repeatmasker.

The assembly genome of the black-footed cat with masked repeat sequences was used to perform gene prediction by homology-based and de novo predictions. Homology-based gene predictions were adopted from the protein sequences of six related species, including of domestic cat (GCA_000181335.5, according to its high-quality of gene-structure's annotation), Asian leopard cat (GCF_016509475.1), tiger (GCF_018350195.1), Canada lynx (GCF_007474595.2), African wild dog (GCF_012295265.1), domestic dog (GCF_014441545.1), and human (GCF_000001405.39), and were aligned with the assembled genome of the BFC using GeMoMa (v1.8) (66, 67) with MMseqs2 v.13.45111 (68) as an alignment tool. All six gene predictions were combined into a final annotation after the filter using GeMoMa annotation filter (GAF) with the parameters of "ce/rce==1" and "iAA>=0.8." Another homology-based gene prediction was made using Genewise (v2.4.1) with default parameters. The homology-based annotated genes were then used for de novo prediction using AUGUSTUS (v3.2.3) (69) and SNAP (v2017-03-01) (70). Finally, EVidenceModeler (71) with biased weights was used to integrate the homology-based and de novo annotated gene models into primary gene models, which were finally filtered for unmatched ones by searching with Pfam (evalue:1e-5) database.

The predicted protein-coding genes were annotated with NCBI non-redundant (NR), UniProt (UniProt and TrEMBL), and eggNOG-mapper databases using diamond command with default parameters. Gene ontology (GO) and KEGG items were annotated by searching with eggnog-mapper.

Whole-Genome Alignment. The genomes of seven *Felis* species (jungle cat, BFC, sand cat, European wildcat, Asian wildcat, Chinese mountain cat, and North African wildcat) with an outgroup of Asian leopard cat were used to align with the domestic cat genome using LAST software (v980, "-P8 -m100 -E0.05") (72). Then, the programme Multiz (v11.2) (73) was used to integrate eight whole genome alignments into a multi-sequence alignment of nine taxa.

Phylogenetic Analysis. The genome-wide alignment sequences constructed above were cut into different window sizes, and a maximum likelihood method was used to construct a phylogenetic tree (RAxML v8.2.12) (https://github.com/stamatak/standard-RAxML). The software orthofinder (v2.5.4) (14) was used to identify the one-to-one orthologues among all involved genomes of felids. The nucleotide and protein sequences of one-to-one orthologues were aligned and combined to create an independent data matrix used for phylogenetic tree building.

Dating. The alignment results of the super-sequence constructed above were used as input files to infer divergence times using the MCMCTREE program in the PAML (v4.5) software package (74). The calibrated time nodes were ">1 Mya" for wildcat species, ">1.79 Mya <4.05 Mya" for the split between the domestic cat (=African wildcat) and sand cat, ">4.80 Mya <8.55 Mya" for the split between the domestic cat lineage and the leopard cat lineage, and ">6.19 Mya <12.52 Mya" for the split between the lynx lineage and the leopard cat lineage, based on previously published calibrations (10).

Introgression Tests. Both Dsuite (v 0.4 r41) (11) and QuIBL (12) were used to detect potential introgressions among *Felis* species. The resequencing samples of *Felis* individuals were mapped onto the reference domestic cat genome (75) and samtools/bcftools (76) were used to call the whole-genome SNPs, which were filtered with the "-i INFO/DP>1000" and then Dsuite was employed to perform the Patterson's D-statistics (ABBA-BABA tests). The assumption of P1, P2, and P3 with an outgroup (O) followed by (((P, P2), P3), O) was used to detect potential introgression between P3 and P2 or P3 and P1. Finally, we filtered the trios that violated this assumption and classified significant introgression with $Z > 2$ (or $P < 0.05$) and others not significant defined as weak introgression.

QuIBL took a strategy using branch lengths, and species triplet topologies of the constructed local Maximum Likelihood (ML) trees of the alignments of the sliding-windows sequences. We conducted QuIBL programme on the detected species triplets with the parameters (Asian leopard cat as the outgroup and numsteps: 50). QuIBL takes the results of mixprop1 as ILS and mixprop2 as introgression by comparing branch lengths. To detect the triplet of domestic cat, BFC, and jungle cat, we used a total of 19,690 local ML trees of whole genome level to distinguish between ILS and introgression. We detected the triplet of jungle cat, sand cat, and BFC with 21,726 local ML trees as the input datasets.

Gene Family Analysis. The protein sequences obtained from the five genomes with high-quality assemblies: jungle cat, BFC, domestic cat and two outgroups, Canada lynx and Asian leopard cat, were used to perform multiple alignments using orthofinder pipeline (v2.5.4) (14), and the identified gene family file was used as the input file. Café (v4.2) (77) was used to test for significantly ($P = 0.05$) expanded or contracted gene families, and the results were displayed with FigTree (v1.2.2).

Positively Selected Genes in BFC. One-to-one orthologues identified by the orthofinder programme (v2.5.4) (14) were used to identify positive selective evolution and rapid evolution using codeml in PAML (v4.5) (74). For the branch model, we performed the one-ratio model and two-ratio model, which were used to test for rapid evolution at the test branch. For the test model, the branch site model was used to test for positive selection. Finally, a chi-square test was used to test for significance, of which "$P \leq 0.05$ and $P \leq 0.01$" were defined as significant and highly significant, respectively.

Quality Filtering, Variant Calling, and Genotyping. The reads of the studied species were mapped to the reference genome using Burrows-Wheeler Aligner (bwa) mem (v0.7.17-r1188) (64) and samtools (v1.8) (76), and then transformed, sorted to remove redundancies. SNPs calling within all genomic alignments was performed using the command HaplotypeCaller and GenotypeGVCFs of the Genome Analysis ToolKit package v3.8 (78) and then was filtered using the VariantFiltration command with the following criteria: "QD < 4.0; FS > 60.0; MQ < 40.0; MQRankSum < −12.5; ReadPosRankSum < −8.0; SOR > 3.0." Individual genotypes were screened to eliminate those with read depths falling below one-third or exceeding twice the mean read depth for that specific individual.

Genetic Diversity Analysis of BFC. The F_{ST} statistic was employed to identify potential genomic differentiation between the BFC and other *Felis* species. First, the above VCF calling method was used to construct genome-wide SNPs in a VCF file between the BFC and the other seven *Felis* species (jungle cat, sand cat, European wildcat, Asian wildcat, Chinese mountain cat, North African wildcat, and domestic cat). Then, a sliding-window approach of 50-kb sliding windows (step = 25 kb) was applied to the genome-wide SNPs in the VCF file to quantify genetic differentiation (F_{ST}) using the VCFtools (v0.1.16) (79) with the parameters "-window-pi 50000 -window-pi-step 25000." We then calculated F_{ST} values and the top 1% and 5% of regions were identified as significant selection regions. The genes in the region of top 5% *Fst* and pairwise nucleotide diversity ($\theta\pi$) were defined as selection genes and used for further study. Tajima's D test was also applied to detect selection with the parameter settings of "–TajimaD 50000 --max-missing 0.9."

Heterozygosity and ROHs Estimates. ROH analysis was performed using Plink (v1.90b6.26) (80) with the normal settings of the parameters (--homozyg -homozyg-window-snp 20 -homozyg-density 50 -homozyg-kb 50) following the method described in the studies (81, 82). The assessment of genome-wide heterozygosity involved calculating the proportion of heterozygous sites in the reference genome using Plink, with the "--het" parameter. FROHs were calculated as the total length of ROH within an individual over the length of the reference genome.

Demographic History Analysis. PSMC (version 0.6.5-r67) was applied to assess changes in effective population size (*Ne*) of the BFCs, relative to other *Felis* spp. (jungle cat, sand cat, African wildcat, Chinese mountain cat, domestic cat, European wildcat, and Asian wildcat). The individuals with a high sequencing depth were selected to ensure the quality of the consensus sequence. We processed quality-trimmed Illumina sequences for each *Felis* spp. by aligning them

to their respective genome assemblies using the bwa with default parameters. To determine average mapping coverage and identify and filter nucleotide variants, samtools was employed. The parameters of the PMSC test were set as -N25, t15, -r5, -p "4 + 25*2 + 4+6". Here, we assume that the mutation rate of the *Felis* spp. as 0.86e-8 and the generation time as 2 y (83). We assessed the consistency of the PSMC tests by conducting 100 bootstrap replicates.

Deleterious Mutation. SnpEff v5.0 (75) and SIFT (https://sift.bii.a-star.edu.sg/) were used to identify high-confidence deleterious mutations. First, variants leading to a functional change are candidates for deleterious mutations. We mainly used snpEff for the functional annotation of each variant. For the preparation of the assembly of genomic, protein-coding-genes annotation and the genome-wide SNPs in the VCF file are needed. First, the annotation file of the BFC was annotated in a "gff" file, which was then transformed into a "gtf" file with the programme of gffread from cufflinks packages. Second, the reference assembly of the BFC genome and the genome-wide SNPs were also prepared. The results of snpEff were mainly categorised into four types: "high" (with stop-gain or frameshift variant), "moderate" (with missense variant or in-frame deletion), "low" (with synonymous variant), and "modifier" (with exon variant or downstream gene variant).

SIFT online was used to predict whether amino acid substitutions affect protein function based on homology and the physical properties of amino acids. Scores of less than 0.05 were usually identified as probably affecting protein function.

Species Distribution Modeling. We applied the method of MAXENT (84), which is a computer program rooted in the principle of maximum entropy from statistical mechanics and information theory, to perform the modeling of species' geographic distributions. To project whether a region that meet the conditions to the ecological niche requirements of the target species. The "presence-only" distribution data of the BFC were obtained from the GBIF database (https://www.gbif.org/zh/) and the environmental data of the LGM period sourced from the Paleoclim database (http://www.paleoclim.org/). These data were used to project the potential habitat of the BFC and explore their potential response to climate change.

Data, Materials, and Software Availability. Both raw FASTQ sequences (accession numbers: SAMN34164677, SAMN34164678, and SAMN37521773-SAMN37521781) and the reference genome assembly (accession number: JAVSGG000000000) (85) of the black-footed cat have been deposited and released in the NCBI database under BioProject accession number PRJNA955150. The major codes used in this research are available at the GitHub repository (https://github.com/GanglabSnnu/bfcproj) (86).

ACKNOWLEDGMENTS. This work was supported by the National Natural Science Foundation of China 31970391 (G.L.), the Natural Science Basic Research Program of Shaanxi 2020JM-280 (G.L.), the Fundamental Research Funds for the Central Universities GK201902008 (G.L.), the Guangzhou Collaborative Innovation Center on Science-tech of Ecology and Landscape Program 202206010058 (W.C.), and NSF grant DEB-1753760 (W.M.). We would like to thank National Engineering Laboratory for Resource Developing of Endangered Chinese Crude Drugs in Northwest China, Shaanxi Normal University. We would also like to thank Ke Shao from Dali University for painting the picture of the black-footed cat. We are grateful to the CryoArks Biobank at National Museums Scotland for supplying nine muscle tissue samples of the BFC.

Author affiliations: [a]College of Life Sciences, Shaanxi Normal University, Xi'an 710119, China; [b]Department of Natural Sciences, National Museums Scotland, Edinburgh EH1 1JF, United Kingdom; [c]School of Geosciences, University of Edinburgh, Edinburgh EH9 3PX, United Kingdom; [d]Hendersonville, NC 28792; [e]Key Laboratory of Vertebrate Evolution and Human Origins of Chinese Academy of Sciences, Institute of Vertebrate Paleontology and Paleoanthropology, Chinese Academy of Sciences, Beijing 100044, China; [f]QinLing-Bashan Mountains Bioresources Comprehensive Development Collaborative Innovation Center, School of Bioscience and Engineering, Shaanxi University of Technology, Hanzhong 723099, China; [g]Guangzhou Zoo, Guangzhou Wildlife Research Center, Guangzhou 510070, China; [h]Xi'an Haorui Genomics Technology Co., Ltd., Xi'an 710116, China; [i]School of Life Science and Technology, Xi'an Jiaotong University, Xi'an 710049, China; and [j]Veterinary Integrative Biosciences, Texas A&M University, College Station, TX 77843

Author contributions: G.L. designed research; J.Y. performed research; J.Y., A.C.K., L.B.L., T.S., Q.J., Y.T., L.Z., P.Y., G.W., C.H., J.W., W.H., Y.L., W.C., D.M., and W.M. analyzed data; A.C.K. provided the samples and revised the manuscript; T.S. revised the manuscript; Q.J. and Y.L. revised the manuscript; W.C. provided the samples; D.M. supported the genome sequencing; W.M. provided the sample and revised the manuscript; and J.Y. and G.L. wrote the paper.

1. A. Kitchener, *The Natural History of the Wild Cats* (Comstock Pub, Associates, 1991).
2. A. Sliwa, "*Felis nigripes*" in *The Mammals of Africa*, J. K. A. M. Hoffmann, Ed. (Bloomsbury Publishing, London, 2013), vol. Carnivores, Pangolins, Equids and Rhinoceroses.
3. A. Sliwa, M. Herbst, M. Mills, Black-footed cats (*Felis nigripes*) and African wild cats (*Felis silvestris*): A comparison of two small felids from South African arid lands. *Biol. Conserv. Wild Felids* 537–558 (2010).
4. A. Sliwa, B. Wilson, M. Kusters, A. Tordiffe, *Felis nigripes. The IUCN Red List of Threatened Species 2016: e. T8542A50652196* (IUCN, Gland, Switzerland, 2016).
5. G. Olbricht, A. Sliwa, In situ and ex situ observations and management of Black-footed cats *Felis nigripes*. *Intern. Zoo YearBook* **35**, 81–89 (1997).
6. B. Eggers, "Evaluation of two different doses of butorphanol–medetomidine–midazolam for anaesthesia in free-ranging versus captive black-footed cats (*Felis nigripes*)," MSc dissertation, University of Pretoria (2016).
7. B. Eggers *et al.*, Evaluation of two doses of butorphanol–medetomidine–midazolam for the immobilization of wild versus captive black-footed cats (*Felis nigripes*). *J. Zoo Wildlife Med.* **51**, 497–506 (2020).
8. K. A. Terio, T. O'Brien, N. Lamberski, T. R. Famula, L. Munson, Amyloidosis in black-footed cats (*Felis nigripes*). *Vet. Pathol.* **45**, 393–400 (2008).
9. H. B. Andervont, T. B. Dunn, Amyloidosis in wild house mice during inbreeding and in hybrids derived from inbred strains and wild mice. *J. Natl. Cancer Inst.* **44**, 719–727 (1970).
10. G. Li, B. W. Davis, E. Eizirik, W. J. Murphy, Phylogenomic evidence for ancient hybridization in the genomes of living cats (Felidae). *Genome Res.* **26**, 1–11 (2016).
11. M. Malinsky, M. Matschiner, H. Svardal, Dsuite-fast D-statistics and related admixture evidence from VCF files. *Mol. Ecol. Res.* **21**, 584–595 (2021).
12. N. B. Edelman *et al.*, Genomic architecture and introgression shape a butterfly radiation. *Science* **366**, 594–599 (2019).
13. T. S. Korneliussen, A. Albrechtsen, R. Nielsen, ANGSD: Analysis of next generation sequencing data. *BMC Bioinform.* **15**, 356 (2014).
14. D. M. Emms, S. Kelly, OrthoFinder: Phylogenetic orthology inference for comparative genomics. *Genome Biol.* **20**, 1–14 (2019).
15. R. I. Popock, *Catalogue of the genus Felis* (British Museum Natural History, London, 1951).
16. G. T. Huang, J. J. Rosowski, M. E. Ravicz, W. T. Peake, Mammalian ear specializations in arid habitats: Structural and functional evidence from sand cat (*Felis margarita*). *J. Comp. Physiol. A Neuroethol Sens Neural. Behav. Physiol.* **188**, 663–681 (2002).
17. G. Peters, L. Baum, M. K. Peters, B. Tonkin-Leyhausen, Spectral characteristics of intense mew calls in cat species of the genus *Felis* (Mammalia: Carnivora: Felidae). *J. Ethol.* **27**, 221–237 (2009).
18. M. Ueda, Y. Ando, Recent advances in transthyretin amyloidosis therapy. *Transl. Neurodegener.* **3**, 19 (2014).
19. D. R. Jacobson, J. N. Buxbaum, A double-variant transthyretin allele (Ser 6, Ile 33) in the Israeli patient "SKO" with familial amyloidotic polyneuropathy. *Hum. Mutat.* **3**, 254–260 (1994).
20. A. Lim *et al.*, Characterization of transthyretin variants in familial transthyretin amyloidosis by mass spectrometric peptide mapping and DNA sequence analysis. *Anal Chem.* **74**, 741–751 (2002).
21. A. De Lillo *et al.*, Epigenetic profiling of Italian patients identified methylation sites associated with hereditary transthyretin amyloidosis. *Clin. Epigenet.* **12**, 1–12 (2020).
22. Y. Ando *et al.*, Guideline of transthyretin-related hereditary amyloidosis for clinicians. *Orphanet J. Rare Dis.* **8**, 1–18 (2013).
23. P. Teilhard de Chardin, P. Leroy, Les Felides de China. *Peking: Pub. Inst. Geobiol.* **11**, 580 (1945).
24. K. Zhang, X. Shen, K. Liu, H. Jiang, Q. Jiangzuo, The modern classification of Felidae –combining molecular phylogeny framework and fossil evidence. *Chin. J. Zool.* **58**, 1–29 (2023), 10.13859/j.cjz.202301001.
25. S. Mukherjee *et al.*, Ecology driving genetic variation: A comparative phylogeography of jungle cat (Felis chaus) and leopard cat (*Prionailurus bengalensis*) in India. *PloS One* **5**, e13724 (2010).
26. A. Sliwa, Home range size and social organisation of black-footed cats. *Mammalian Biol.* **69**, 96–107 (2004).
27. H. Hemmer, P. Grubb, C. Groves, Notes on the sand cat, *Felis margarita* Loche, 1858. *Z. Säugetierkd.* **41**, 286–303 (1976).
28. G. J. Linares Matás, J. J. W. A. Yravedra, 'We hunt to share': Social dynamics and very large mammal butchery during the Oldowan–Acheulean transition **53**, 224–254 (2021).
29. S. Dominici, Taphonomy and paleoecology of shallow marine macrofossil assemblages in a collisional setting (late Pliocene–early Pleistocene, western Emilia, Italy). *Palaios* **16**, 336–353 (2001).
30. P. Huybers, W. Curry, Links between annual, Milankovitch and continuum temperature variability. *Nature* **441**, 329–332 (2006).
31. G. Crippa, A. Baucon, F. Felletti, G. Raineri, D. Scarponi, A multidisciplinary study of ecosystem evolution through early Pleistocene climate change from the marine Arda River section, Italy. *Quaternary Res.* **89**, 533–562 (2018).
32. B. Kurtén, On the evolution of the European wild cat, *Felis silvestris* Schreber. *Acta Zoologica Fennica* **111**, 1–26 (1965).
33. P. U. Clark *et al.*, The middle Pleistocene transition: Characteristics, mechanisms, and implications for long-term changes in atmospheric pCO2. *Quaternary Sci. Rev.* **25**, 3150–3184 (2006).
34. R. Seidl *et al.*, Globally consistent climate sensitivity of natural disturbances across boreal and temperate forest ecosystems. *Ecography* **43**, 967–978 (2020).
35. J. A. Serpell, "Domestication and history of the cat" in *The Domestic Cat: The Biology of its Behaviour*, D. C. Turner, P. Bateson, Eds. (Cambridge University Press, Cambridge, United Kingdom, 2000), vol. 2, pp. 180–192.
36. K. Nowell, P. Jackson, *Wild Cats: Status Survey and Conservation Action Plan* (IUCN Gland, 1996), vol. 382.

37. M. J. Daniels *et al.*, Ecology and genetics of wild-living cats in the north-east of Scotland and the implications for the conservation of the wildcat. *J. Appl. Ecol.* **38**, 146–161 (2001).
38. J. F. Kamler *et al.*, Ecological relationships of black-footed cats (*Felis nigripes*) and sympatric canids in South Africa. *Mammalian Biol.* **80**, 122–127 (2015).
39. M. Cartmill, New views on primate origins. *Evol. Anthropol. Issues, News, and Rev.* **1**, 105–111 (1992).
40. L. Crompton, G. A. Doyle, M. Kaylzard, *Creatures of the Dark: The Nocturnal Prosimians* (Plenum Press, 1995).
41. K. N. Alagramam *et al.*, The mouse Ames waltzer hearing-loss mutant is caused by mutation of Pcdh15, a novel protocadherin gene. *Nat. Genet.* **27**, 99–102 (2001).
42. J. Nathans, D. Thomas, D. S. Hogness, Molecular genetics of human color vision: The genes encoding blue, green, and red pigments. *Science* **232**, 193–202 (1986).
43. T. Eisenberger *et al.*, A C-terminal nonsense mutation links *PTPRQ* with autosomal-dominant hearing loss, *DFNA73*. *Genet Med.* **20**, 614–621 (2018).
44. T. Walsh *et al.*, Whole exome sequencing and homozygosity mapping identify mutation in the cell polarity protein GPSM2 as the cause of nonsyndromic hearing loss *DFNB82*. *Am. J. Hum. Genet* **87**, 90–94 (2010).
45. H. Azaiez *et al.*, HOMER2, a stereociliary scaffolding protein, is essential for normal hearing in humans and mice. *PLoS Genet.* **11**, e1005137 (2015).
46. R. L. P. Santos-Cortez *et al.*, Identification of novel candidate genes and variants for hearing loss and temporal bone anomalies. *Genes (Basel)* **12**, 566 (2021).
47. N. Hilgert, R. J. Smith, G. Van Camp, Function and expression pattern of nonsyndromic deafness genes. *Curr. Mol. Med.* **9**, 546–564 (2009).
48. E. D. Lynch *et al.*, Nonsyndromic deafness *DFNA1* associated with mutation of a human homolog of the Drosophila gene diaphanous. *Science* **278**, 1315–1318 (1997).
49. P. Li *et al.*, Exogenous L-carnitine ameliorates burn-induced cellular and mitochondrial injury of hepatocytes by restoring CPT1 activity. *Nutrit. Metab.* **18**, 1–12 (2021).
50. J. Calvo *et al.*, Isolation, mapping and identification of SNPs for four genes (*ACP6*, *CGN*, *ANXA9*, *SLC27A3*) from a bovine QTL region on BTA3. *Cytogenet. Genome Res.* **114**, 39–43 (2006).
51. M. K. Montgomery *et al.*, Hexosaminidase A (*HEXA*) regulates hepatic sphingolipid and lipoprotein metabolism in mice. *FASEB J.* **35**, e22046 (2021).
52. Y. Soreze *et al.*, Mutations in human lipoyltransferase gene *LIPT1* cause a Leigh disease with secondary deficiency for pyruvate and alpha-ketoglutarate dehydrogenase. *Orphanet J. Rare Dis.* **8**, 192 (2013).
53. F. Tort *et al.*, Mutations in the lipoyltransferase *LIPT1* gene cause a fatal disease associated with a specific lipoylation defect of the 2-ketoacid dehydrogenase complexes. *Hum. Mol. Genet* **23**, 1907–1915 (2014).
54. I. Rudan *et al.*, Inbreeding and risk of late onset complex disease. *J. Med. Genet.* **40**, 925–932 (2003).
55. M. Fareed, M. Afzal, Genetics of consanguinity and inbreeding in health and disease. *Ann. Hum. Biol.* **44**, 99–107 (2017).
56. M. Lee *et al.*, Systematic computational identification of variants that activate exonic and intronic cryptic splice sites. *Am. J. Hum. Genet.* **100**, 751–765 (2017).
57. Z. Wang, C. B. Burge, Splicing regulation: From a parts list of regulatory elements to an integrated splicing code. *RNA* **14**, 802–813 (2008).
58. R. Vassar, *BACE1* inhibitor drugs in clinical trials for Alzheimer's disease. *Alzheimer's Res. Therapy* **6**, 1–14 (2014).
59. X. Zhang, W. Song, The role of *APP* and *BACE1* trafficking in APP processing and amyloid-β generation. *Alzheimer's Res. Therapy* **5**, 1–8 (2013).
60. O. Dudchenko *et al.*, De novo assembly of the Aedes aegypti genome using Hi–C yields chromosome–length scaffolds. *Science* **356**, 92–95 (2017).
61. O. Dudchenko *et al.*, The Juicebox Assembly Tools module facilitates de novo assembly of mammalian genomes with chromosome-length scaffolds for under $1000. bioRxiv [Preprint] (2018). https://doi.org/10.1101/254797 (Accessed 11 October 2022).
62. M. Kolmogorov, J. Yuan, Y. Lin, P. A. Pevzner, Assembly of long, error-prone reads using repeat graphs. *Nat. Biotechnol.* **37**, 540–546 (2019).
63. M. Seppey, M. Manni, E. M. Zdobnov, "BUSCO: Assessing genome assembly and annotation completeness" in *Gene Prediction: Methods Protocols* (Humana Press, 2019), pp. 227–245.
64. H. Li, Aligning sequence reads, clone sequences and assembly contigs with BWA-MEM. arXiv [Preprint] (2013). https://doi.org/10.48550/arXiv.1303.3997 (Accessed 10 September 2022).
65. H. Li, A statistical framework for SNP calling, mutation discovery, association mapping and population genetical parameter estimation from sequencing data. *Bioinformatics* **27**, 2987–2993 (2011).
66. J. Keilwagen, F. Hartung, M. Paulini, S. O. Twardziok, J. Grau, Combining RNA-seq data and homology-based gene prediction for plants, animals and fungi. *BMC Bioinform.* **19**, 1–12 (2018).
67. J. Keilwagen *et al.*, Using intron position conservation for homology-based gene prediction. *Nucleic Acids Res.* **44**, e89–e89 (2016).
68. M. Steinegger, J. Söding, MMseqs2 enables sensitive protein sequence searching for the analysis of massive data sets. *Nat. Biotechnol.* **35**, 1026–1028 (2017).
69. M. Stanke, M. Diekhans, R. Baertsch, D. Haussler, Using native and syntenically mapped cDNA alignments to improve de novo gene finding. *Bioinformatics* **24**, 637–644 (2008).
70. I. Korf, Gene finding in novel genomes. *BMC Bioinform.* **5**, 1–9 (2004).
71. B. J. Haas *et al.*, Automated eukaryotic gene structure annotation using EVidenceModeler and the program to assemble spliced alignments. *Genome Biol.* **9**, 1–22 (2008).
72. S. M. Kiełbasa, R. Wan, K. Sato, P. Horton, M. C. Frith, Adaptive seeds tame genomic sequence comparison. *Genome Res.* **21**, 487–493 (2011).
73. M. Blanchette *et al.*, Aligning multiple genomic sequences with the threaded blockset aligner. *Genome Res.* **14**, 708–715 (2004).
74. Z. Yang, PAML 4: Phylogenetic analysis by maximum likelihood. *Mol. Biol. Evol.* **24**, 1586–1591 (2007).
75. K. R. Bredemeyer *et al.*, Ultracontinuous single haplotype genome assemblies for the domestic cat (Felis catus) and Asian leopard cat (*Prionailurus bengalensis*). *J. Heredity* **112**, 165–173 (2021).
76. H. Li *et al.*, The sequence alignment/map format and SAMtools. *Bioinformatics* **25**, 2078–2079 (2009).
77. T. De Bie, N. Cristianini, J. P. Demuth, M. W. Hahn, CAFE: A computational tool for the study of gene family evolution. *Bioinformatics* **22**, 1269–1271 (2006).
78. A. McKenna *et al.*, The genome analysis toolkit: A mapreduce framework for analyzing next-generation DNA sequencing data. *Genome Res.* **20**, 1297–1303 (2010).
79. P. Danecek *et al.*, The variant call format and VCFtools. *Bioinformatics* **27**, 2156–2158 (2011).
80. S. Purcell *et al.*, PLINK: A tool set for whole-genome association and population-based linkage analyses. *Am. J. Hum. Genet.* **81**, 559–575 (2007).
81. M. Bosse *et al.*, Regions of homozygosity in the porcine genome: Consequence of demography and the recombination landscape. *PLoS Genet.* **8**, e1003100 (2012).
82. P. Dobrynin *et al.*, Genomic legacy of the African cheetah, *Acinonyx jubatus*. *Genome Biol.* **16**, 277 (2015).
83. R. J. Wang *et al.*, De novo mutations in domestic cat are consistent with an effect of reproductive longevity on both the rate and spectrum of mutations. *Mol. Biol. Evol.* **39**, msac147 (2022).
84. S. J. Phillips, R. P. Anderson, R. E. Schapire, Maximum entropy modeling of species geographic distributions. *Ecol. Modell.* **190**, 231–259 (2006).
85. J. Yuan *et al.*, The genome of the black-footed cat: Revealing a rich natural history and urgent conservation priorities for small felids. National Center for Biotechnology Information: SAMN34164677, SAMN34164678, SAMN37521773-SAMN37521781, JAVSGG000000000. NCBI. https://www.ncbi.nlm.nih.gov/bioproject/955150. Deposited 13 April 2023.
86. J. Yuan *et al.*, The genome of the black-footed cat: Revealing a rich natural history and urgent conservation priorities for small felids. GitHub: https://github.com/GanglabSnnu/bfcproj. Deposited 5 September 2023.